



Case study of slab bridges

Estudo de caso de pontes de laje

DOI: 10.56238/isevmjv2n6-003

Receipt of originals: 10/11/2023

Approved on: 11/28/2023

Fernando Xavier P. L. Talavera

Undergraduate student of the Civil Engineering course – IFSP, Votuporanga Campus

Gustavo Cabrelli Nirschl

Master Professor of the Department of Civil Engineering – IFSP, Votuporanga Campus

ABSTRACT

The article introduces the central theme with a brief explanation of the historical evolution of bridges, highlighting the materials and construction methods used in each period. It also provides a summary of each type of bridge and construction methods used throughout the evolution of engineering. In addition, the present work includes analyses of case studies that address the design of slab bridges, performing a bibliographic review of the academic works already carried out, making a comparison with the pre-design guidelines proposed in the DNER Special Works of Arts Design Manual. The results indicate that the thickness of the slabs recommended in the manual resulted in larger structural dimensions than those used in the case studies, but following the same order of magnitude. In addition, the steel rates used in the bridge slabs were calculated, whose values were close to a value in the technical literature.

Keywords: Slab bridges, Case study, Pre-dimensioning, Steel rates.

1 INTRODUCTION

According to NBR 7188:2013, bridges are constructions used to overcome natural obstacles, such as rivers, streams and valleys, and are subject to the action of moving loads with variable positioning.

According to Chianca (2016), the first records of the use of bridges in history, taking into account the connections of the supports with the ground, were made from the third century BC, built by the Romans; later, during the 5th to 15th centuries AD, bridges were discovered for numerous purposes, including military, commercial, residential, and aqueducts.

Also according to Chianca (2016), later, with the advent of the Industrial Revolution, there was an important technological advance in the development of new bridges, opening up wider design possibilities, due to new machinery, materials and construction methods.

According to Leonhardt (1979), cited by El Debs and Takeya (2007), historically and chronologically, bridges have evolved as follows:



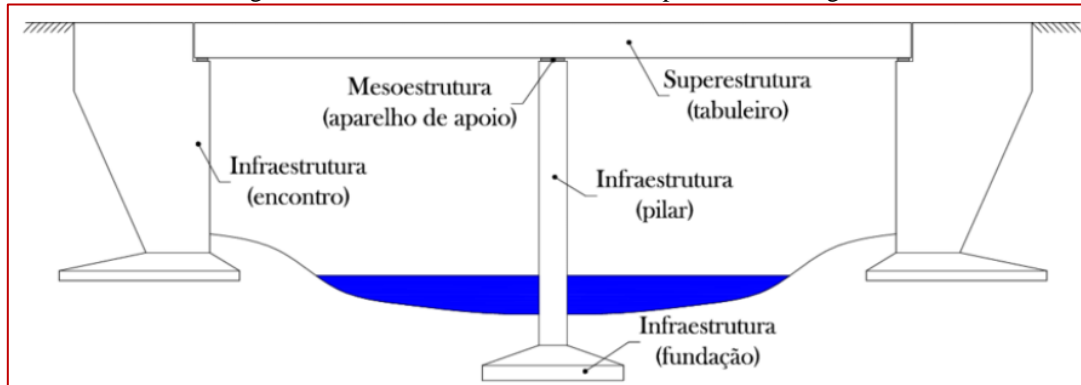
- **Wooden bridges** - Wood has been employed since antiquity in the construction of bridges, initially with fairly simple structural arrangements. It is noteworthy that, with this material, bridges with considerable spans were built, such as the one built in 1758, over the Rhine River, with a span of 118 m.
- **Stone bridges** - stone, like wood, has been used since ancient times in the construction of bridges. The Romans and Chinese were already building stone vaults before Christ. The Romans even built bridges, in the form of a semicircular arch with up to 30 m span. In the Middle Ages, they reached spans of 50 m.
- **Metal bridges** - although the first metal bridges appeared at the end of the eighteenth century, in cast iron, it was from the middle of the following century, with the development of the railways, that the use of steel in the construction of bridges flourished.
- **Reinforced concrete bridges** - the first concrete bridges appeared in the early 20th century. They were simple concrete bridges in a tri-articulated arch, with the material replacing the stone, and it was from 1912 that the construction of girder and gantry bridges in reinforced concrete, with spans of up to 30 m, began to be built.
- **Prestressed concrete bridges** - although the first prestressed concrete bridges were built from 1938 onwards, it was after World War II that prestressed concrete began to be used with great frequency, because of the need to quickly rebuild many bridges destroyed during the war.

According to Pinho and Bellei (2007), numerous types of bridges are possible. Basically, the structures of today's bridges and viaducts can be constructed of concrete, wood, steel, and steel-concrete composite structures. These authors mention that, currently, the structural engineer has at his disposal a great power of analysis with the use of computer programs, developing in a short time projects that would take months or years.

2 STRUCTURAL ELEMENTS OF BRIDGES

According to the structural aspects, the bridges can be divided into superstructure, infrastructure, and support apparatus, as per Figure 1.

Figure 1 - Illustrative scheme of the composition of bridges.



Source: Adapted from El Debs and Takeya (2007)

According to El Debs and Takeya (2007), **the superstructure** is the part of the bridge intended to overcome the obstacle, and can be subdivided into two parts:

- **Main structure** (or main structural system or simply structural system) - which has the function of overcoming the free span;
- **Secondary structure** (or deck or platform) - which receives the direct action of the loads and transmits it to the main structure.

Also according to El Debs and Takeya (2007), **the support apparatus** is the element placed between the infrastructure and the superstructure, intended to transmit the support reactions and allow certain movements of the superstructure.

El Debs and Takeya (2007) mention that **infrastructure** is the part of the bridge that receives the loads of the superstructure through the support apparatus and transmits them to the ground. Infrastructure can be subdivided into supports and foundations. Supports can be subdivided into:

- **Abutment** - element located at the ends of the bridge, in the transition between the bridge and the embankment of the track, and which has the dual function of support and support of the ground;
- **Pillar** - a support element, usually located in the intermediate region, and which does not have the purpose of supporting the ground.

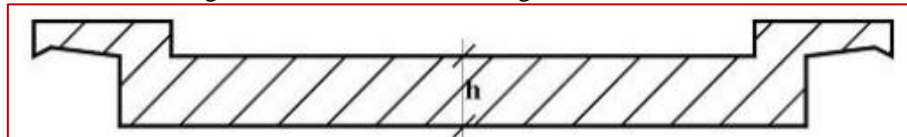
3 TYPES OF SUPERSTRUCTURE

According to the structural system of the superstructure, Vitório (2002) presents some possibilities:

3.1 LASLAB BRIDGE

These are bridges whose decks consist only of slabs, without any type of beam (figure 2). This is the solution adopted only for small spans.

Figure 2 - Cross-section of bridge deck in solid slab.

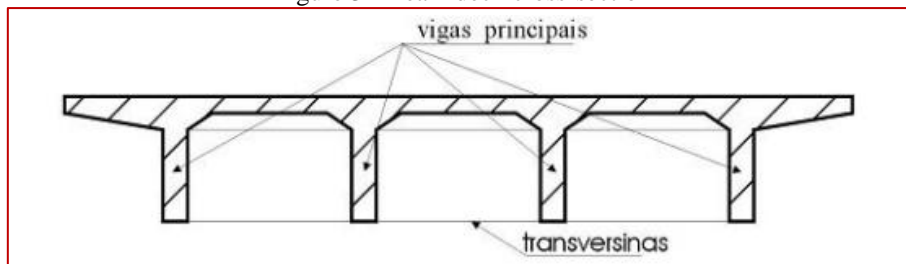


Source: Vitório (2002)

3.2 GIRDER BRIDGE

Bridges whose deck structural system consists of two or more longitudinal girders (stringers) and transverse beams (transversinas). In this type of structure, there is an upper slab on which the runways are located (figure 3).

Figure 3 - Beam deck cross-section

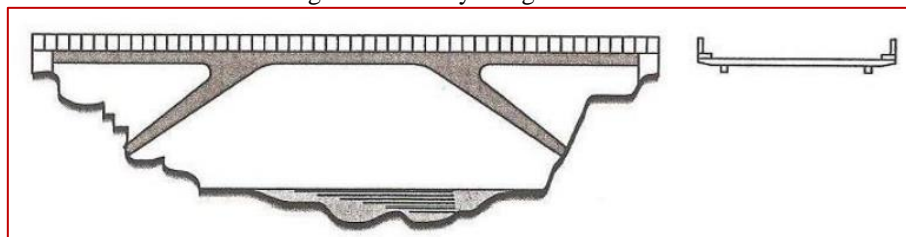


Source: Vitório (2002)

3.3 POTRY BRIDGE

In these types of bridges, the frames are formed by connecting the beams with the pillars or with the walls of the abutments, characterizing the continuity between these elements instead of the joints (figure 4).

Figure 4 - Gantry bridge scheme.



Source: Marchetti (2008)

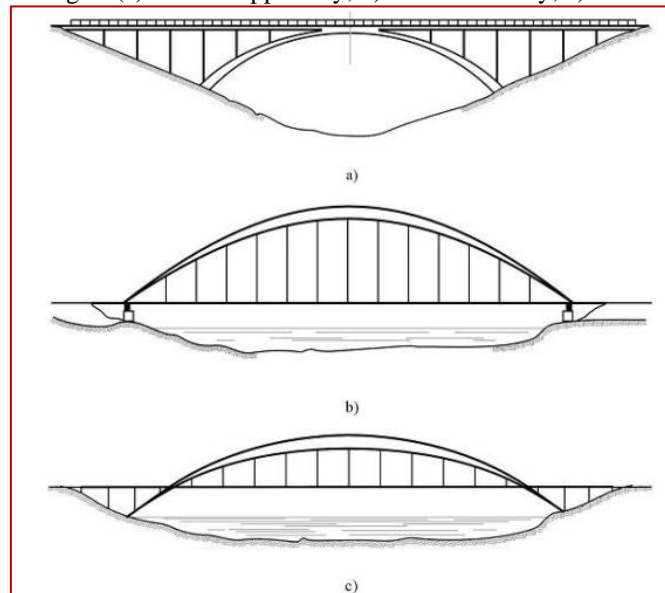
3.4 ARCH BRIDGE

This structural system was widely used in the past because it was the only viable alternative to overcome large spans, especially due to the absence of intermediate supports, making it possible to build over watercourses without the need for submerged pillars.

The predominance of compressive forces with small eccentricity and the requirement of small sections of reinforcements made the arch the appropriate structure for the use of reinforced concrete.

Figure 5 shows three schemes commonly used in arch bridges.

Figure 5 - Arch bridges. (a) with an upper tray; b) with lower tray; c) with intermediate tray.

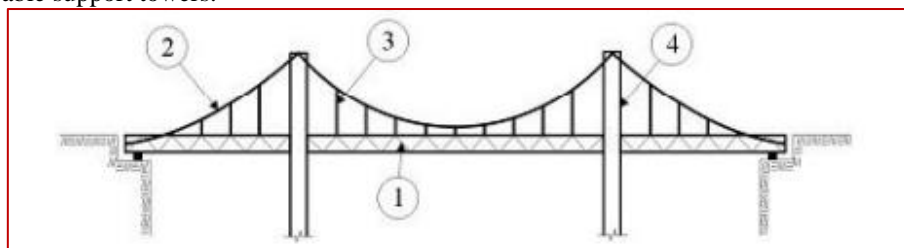


Source: Vitório (2002)

3.5 SUSPENSION BRIDGE

These bridges are constituted and characterized mainly by the presence of parabolically arranged cables and vertical hangings, as can be seen in figure 6, generally executed in metal beams suspended by steel bearing cables.

Figure 6 - Schematic of a suspension bridge. 1. Metal beam; 2. Load-bearing cable; 3. Hanging hanging beam; 4. Load-bearing cable support towers.

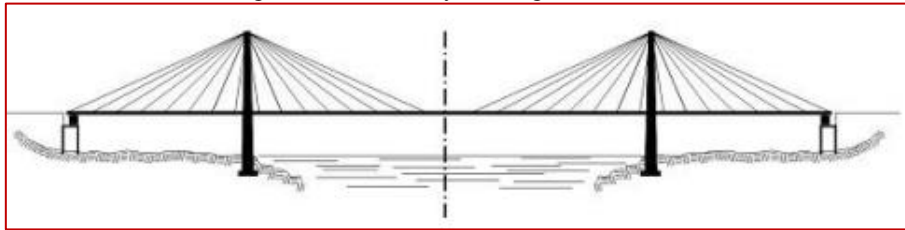


Source: Vitório (2002)

3.6 PONTE ESTAIADA

On cable-stayed bridges, the deck is suspended by means of inclined cables fixed to towers (figure 7). The deck, usually made of metal or prestressed concrete, must have great torsional rigidity, in order to reduce the vibratory movements caused by the transverse action of the wind.

Figure 7 - Cable-stayed bridge with cables.



Source: Vitório (2002)

4 SLAJ BRIDGES

According to NBR 7187 : 2021, the minimum thicknesses in solid slabs must be:

- a) slabs intended for the passage of railway traffic: $H \geq 20$ cm;
- b) slabs intended for the passage of road traffic: $H \geq 15$ cm;
- c) Other cases: $H \geq 12$ cm.

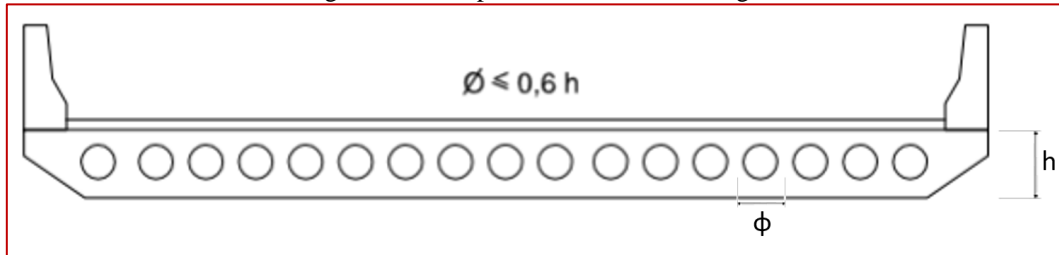
According to the DNER's Special Works of Art Design Manual, in Brazil (1996), slab structures can be cast on site or made up of precast elements, being indicated for short spans, low construction height and small height/span ratios. They have great constructive advantages, since the details of formwork, reinforcement and concreting are simple, resulting in speed and ease of construction.

According to Brasil (1996), for structures cast on site, there are two main types of slabs: solid and hollow. Solid slabs in conventional reinforced concrete are used for spans up to 15 m, with a height/span ratio of around 1/15, in isostatic spans, and 1/20 and 1/24, in continuous spans; In prestressed reinforced concrete, they reach a height/span ratio of 1/30, being used in spans up to 24 m when the height of the slab is constant and spans up to 30 m or 36 m when corbels are introduced in the supports.

According to Brasil (1996), hollow slabs are recommended to reduce the self-weight that structures with large spans would have if they were solid slabs; For spans larger than 12 m, it is advisable to provide longitudinal openings, in general, in a circular shape, as per

figure 8. The minimum thicknesses of the concrete slabs, above and below the voids, should not be less than 12 cm, and the ribs between the voids should have an adequate thickness to accommodate the reinforcements, making the use of stirrups mandatory.

Figure 8 - Example of a hollow slab bridge.

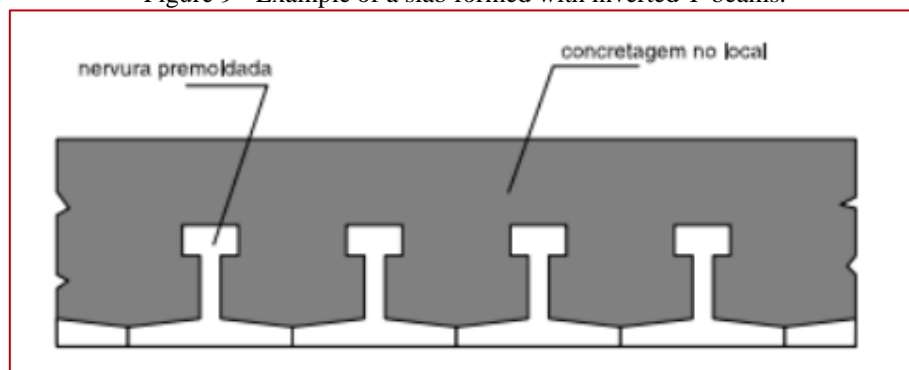


Source: Adapted from Brazil (1996)

Brasil (1996) mentions that, for structures consisting of precast slab elements, we can count on structures with inverted T-beams and those with hollow elements, according to the

Figure 9. Structures with inverted T-beams are placed in their final places and filled with concrete to achieve the desired gravel set. The joint work of the precast elements is guaranteed by waiting reinforcement and transverse reinforcement. This structure is commonly used for spans of 12 to 20 m and the thickness of the precast elements varies from 12 to 15 cm. A variant of this system is a solution in which the voids between the elements are not filled and the concreting is done with the help of formwork. This method is generally used for isostatic spans between 15 and 30 m, with height/span ratio ranging from 1/20 to 1/25 for prestressed precast beams, and the web thickness is between 10 and 20 cm, with the maximum weight of each rib usually less than 30 tf.

Figure 9 - Example of a slab formed with inverted T-beams.



Source: Brazil (1996)

On the other hand, the structures made up of hollow elements, according to Brasil (1996), are composed of precast box beams juxtaposed transversely, with joints filled with mortar and transverse connection made by means of prestressing or passive reinforcement. The lower tables

of the box beams make this system suitable for works with posterior longitudinal continuity. This type of cross-section is used for low height/span ratios of 1/25 or less in prestressed concrete, with a maximum weight of the precast elements not exceeding 70 tf and spans of 15 to 30 m. The height of the deck varies from 0.5 to 1.0 meters, with minimum thicknesses of 12 cm for the table and 10 cm for the web of the beams. It is advisable to provide regularization fillers to level the structure before paving, due to the different deformations of the precast beams.

5 METHODOLOGY

The methodology of this work is based on a literature review and data collection of relevant information about the slab bridges studied, especially regarding the relationship between thickness over the slab span and steel rates, relating to reference values.

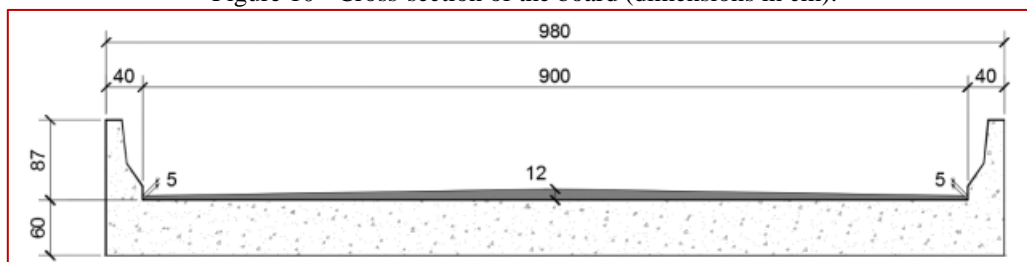
6 RESULTS AND DISCUSSION

6.1 SLAB BRIDGES CASE STUDIES

6.1.1 Ponte Chianca (2016)

Chianca (2016) presents a class 45 road bridge (defined for a type vehicle of 450 kN, with six wheels, according to Andrade (2017)), located on a Class IV single-lane highway (single-lane highway, supporting traffic volumes with a daily traffic volume of less than 300 vehicles, according to DAER (1991)). It has a span with a total length of 11.00 m and a width of 9.80 m, whose total width of the bridge corresponds to two lanes, each 3.0 m wide, in addition to two shoulders of 1.50 m each. The structure of the bridge is supported by two abutments in cyclopean concrete walls at the ends, which were designed taking into account the span and class of the bridge. For the construction of the bridge deck, a solid slab with a constant thickness of 60cm was used. Figures 10 and 11 show the bridge sections.

Figure 10 - Cross-section of the board (dimensions in cm).



Fonte: Chianca (2016)

According to the recommendations of Brazil (1996), described in this article, for the span of 11m, a good pre-dimensioning would be a thickness of $11/15 = 0.73\text{m}$; According to NBR7187:2021, the minimum thickness should be 20cm. Thus, the 60 cm dimensioned by Chianca (2016) is within the expected range.

Figure 11 – Longitudinal section of the board (dimensions in cm).



Fonte: Chianca (2016)

As for the design of flexural reinforcement, Chianca (2016) shows table 1, with no transverse reinforcement being necessary.

Table 1 – Reinforcement from design to bending.

Posição	Momento de Cálculo (tfm/m)	bw (cm)	h (cm)	d (cm)	x (cm)	Domínio	$A_{s,calc}$ (cm/m)	ϕ adotado	Espaçamento (cm)
Meio da Placa Direção x	75.836	100	60	56.25	9.96	2	33.37	ϕ 25.0	15
Meio do Bordo livre Direção x	86.592	100	60	56.25	11.51	2	38.56	ϕ 25.0	12.5
Meio da Placa Direção y	12.836	100	60	54.5	16.36	3	5.48	ϕ 10.0	15

Fonte: Chianca (2016)

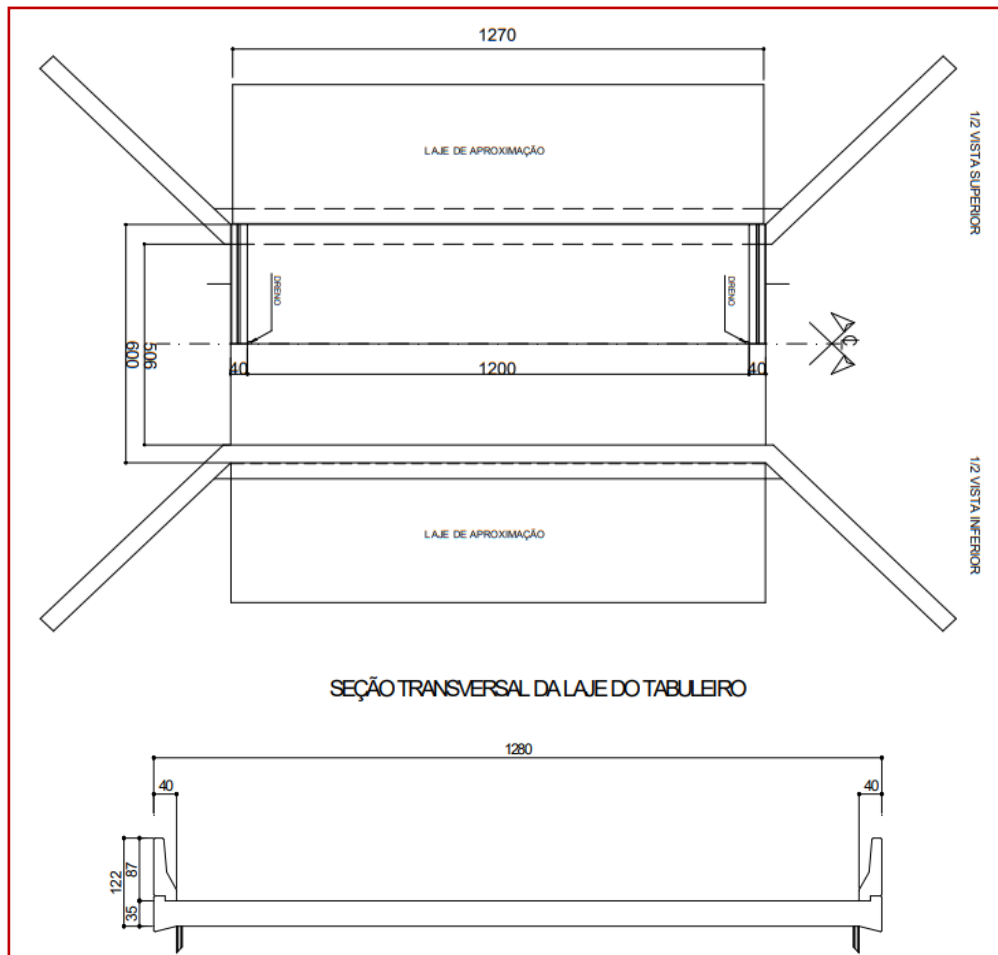
Also according to Chianca (2016), the X direction refers to the direction parallel to the bridge axis and the Y direction to the direction perpendicular to the bridge axis.

6.1.2 Freire Bridge (2013)

Freire (2013) presents an example of a slab bridge with a span of 6.00 m, simply supported on its edges, width of 12.70 m, dimensioned with a thickness value for the slab of 0.35 m, whose plan and cross-section can be seen in figure 12. Using the value suggested in Brazil (1996), we

have a pre-dimensioning value of $6.00/15 = 0.40\text{m}$. Thus, the value of 0.35m is within the expected order of magnitude.

Figure 12 – Plan and cross-section of the model board (dimensions in cm).



Source: Freire (2013)

According to the materials used in the structure (CA-50 steel, $f_y = 500\text{MPa}$, C35 concrete), Freire (2013) designs the following values of flexural reinforcement:

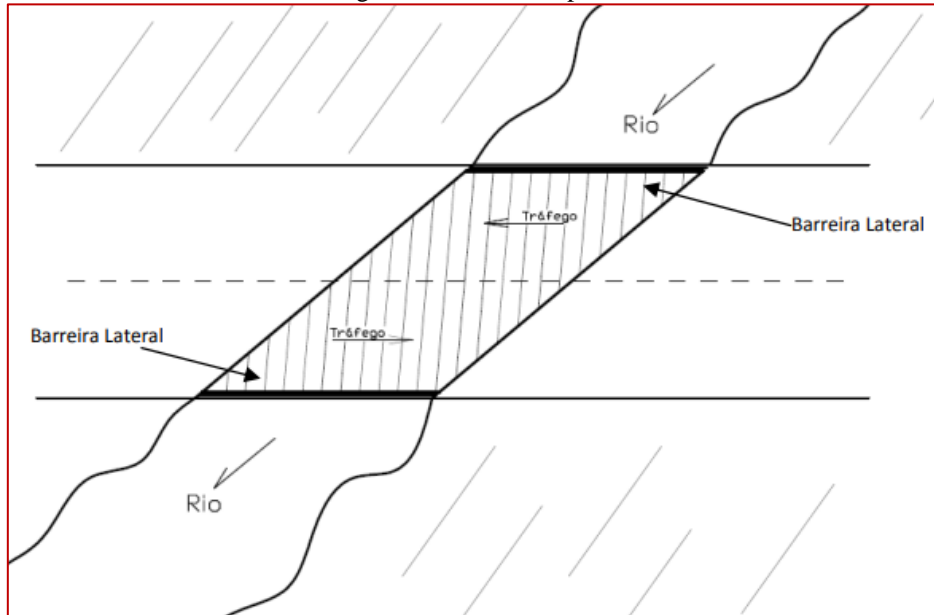
- Parallel to the axis of the bridge: $A_s = 28\text{cm}^2/\text{m}$ – Adopting $\phi 20 \text{ c}/ 10$.
- Perpendicular to the axis of the bridge: $A_s = 5.4 \text{ cm}^2/\text{m}$ – Adopting $\phi 16 \text{ c}/ 30$.

6.1.3 Ponte Daher (2010)

Daher (2010), for a flexural analysis and design project, used a model of a bridge in a solid concealed slab to overcome a river span with 9.65m . In the design, Daher (2010) adopted a thickness of 0.55m . Since it is an isostatic bridge, using the values suggested by Brasil (1996), we would have a thickness of $9.65/15 = 0.64\text{m}$. Therefore, the 0.55 m dimensioned are within the

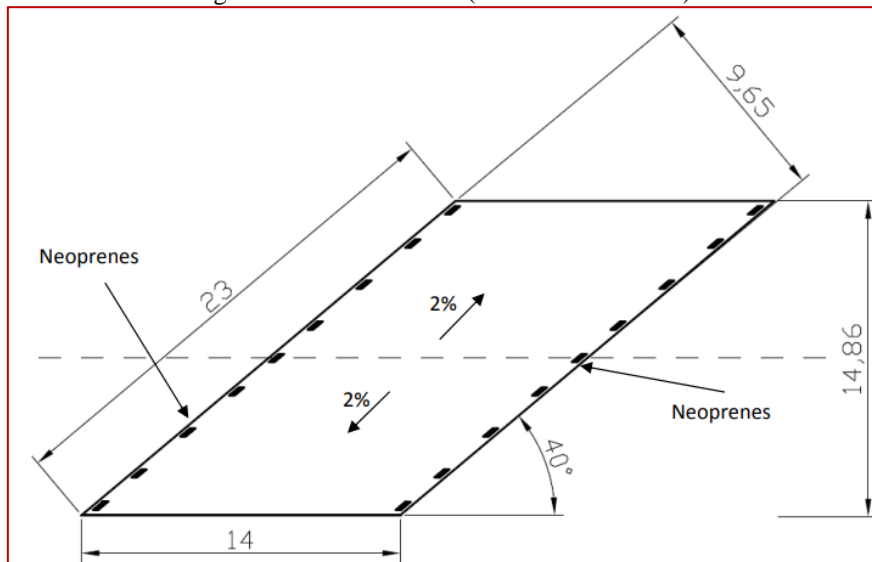
order of magnitude expected in the pre-dimensioning. The bridge deck rests on Neoprene devices, which in turn support each other on the abutments, as shown in the schematic drawings below, shown in figures 13, 14 and 15.

Figure 13 – Situation plan.



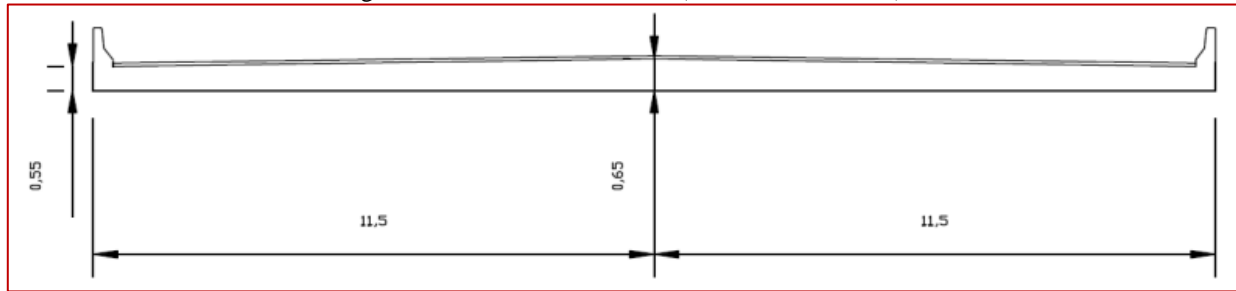
Fonte: Daher (2010)

Figure 14 – Bottom view (measured in meters).



Fonte: Daher (2010)

Figure 15 – Cross-sectional cut (measured in meters).



Fonte: Daher (2010)

Daher (2010) shows, in table 2, the summary of reinforcements, calculated by 3 different methods. Leonhardt's method, according to Parsekian (1996), generates reinforcements that are hidden in relation to the main directions, but orthogonal to each other, based on the criterion of resistance of the normal moment. On the other hand, the Wood & Armer method (90° and 40°), according to Parsekian (1996), allows the design of reinforcement in orthogonal or non-orthogonal meshes, based on the balance of applied and resistant forces of an action.

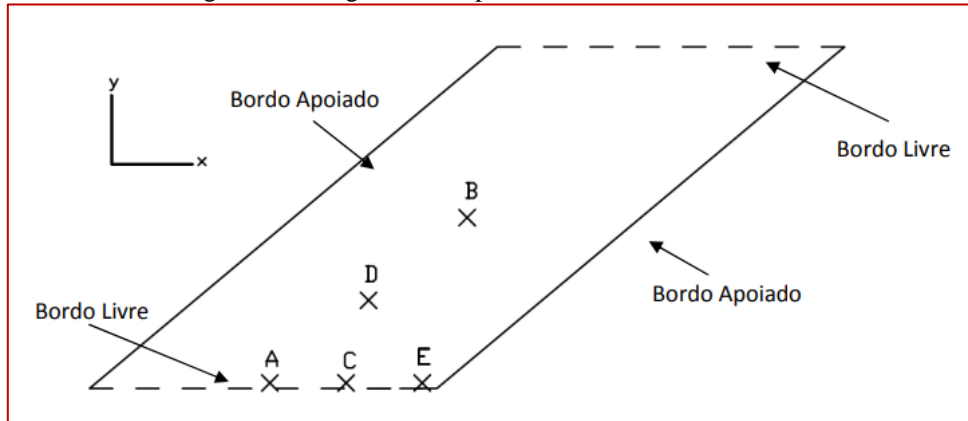
Table 2 – Summary of reinforcement areas (cm²) from design to bending.

(cm ² /m)	Leonhardt		W & A (90°)		W & A (40°)	
	As _x	As _y	As _x	As _y	As _x	As _B
A	30,77	8,81	30,77	8,81	21,42	13,31
B	15,12	17,94	15,12	17,94	37,93	53,55
C	35,90	16,72	35,90	16,72	17,24	24,90
D	20,17	18,39	20,17	18,39	24,14	40,19
E+	9,25	26,94	9,25	26,94	12,62	60,96
E-	33,34	10,70	33,34	10,70	64,53	8,25

Fonte: Daher (2010)

Daher (2010), na Figure 16, displays the locations of each point. Points A and B refer to the places where there is the greatest positive flexural moment in the span of the freeboard region and in the span of the central region, respectively; point E is the place where there is the greatest negative bending moment due to the influence of the bridge conspiracy. On the other hand, points C and D are auxiliary for the calculation.

Figure 16 - Diagram of the points used for the calculation.

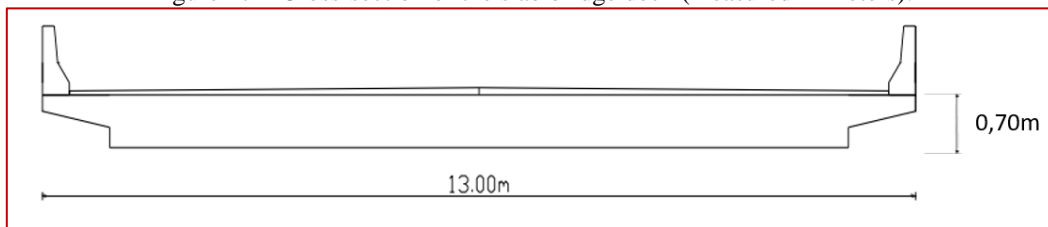


Fonte: Daher (2010)

6.1.4 Gordilho Neto Bridge (2012)

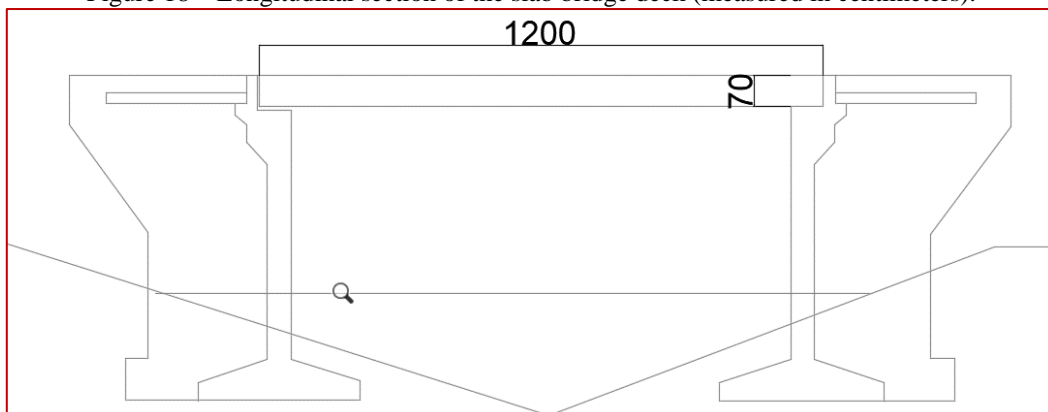
Gordilho Neto (2012), for a comparative analysis of the design via Rüsç tables with the grid method, used a solid slab bridge with a span of 12 meters, supported at the ends, 13 meters wide and 0.70m thick. As it is an isostatic bridge, according to Brasil (2016), we would have a thickness of $12/15 = 0.80\text{m}$, making the thickness adopted in the order of magnitude of the suggested pre-dimensioning. The cross-sectional and longitudinal sections of the bridge can be seen in figure 17 and 18, respectively.

Figure 17 – Cross-section of the slab bridge deck (measured in meters).



Source: Gordilho Neto (2012)

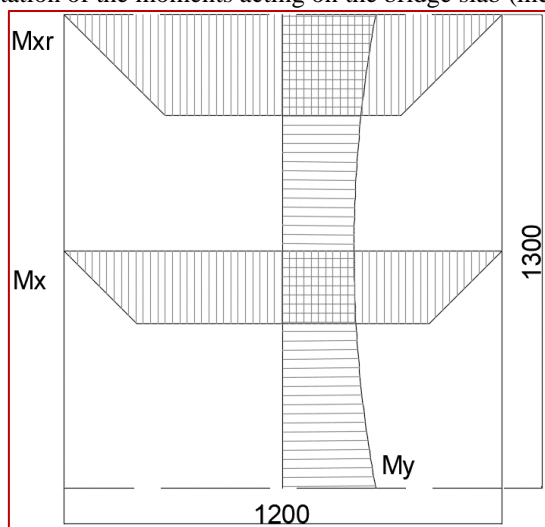
Figure 18 – Longitudinal section of the slab bridge deck (measured in centimeters).



Source: Adapted from Gordilho Neto (2012)

After analyzing the bridge structure using the Rüsç tables and the grid method, Gordilho Neto (2012) arrived at the results of maximum bending moments shown in tables 3 and 4. As shown in figure 19, M_x is the maximum moment in the center of the board, in the direction parallel to the axis, M_y is the maximum moment at the edge of the board, in the direction perpendicular to the axis, and M_{xr} is the maximum moment at the edge of the board, in the direction parallel to the axis.

Figure 19 – Representation of the moments acting on the bridge slab (measured in centimeters).



Source: Author's own (2023)

Table 3 – Maximum bending moments (grid analysis).

Analogia de Grelha	M_x (kN.m)	M_y (kN.m)	M_{xr} (kN.m)
Carregamento Permanente	445,23	-31,58	463,27
Carregamento Móvel no Bordo	248,70	-35,49	367,57
Carregamento Móvel no Centro	268,28	22,96	-

Source: Gordilho Neto (2012)

Table 4 – Maximum bending moments (Rüsç tables).

Tabelas de Rüsç	M_x (kN.m/m)	M_y (kN.m/m)	M_{xr} (kN.m/m)
Carregamento Permanente	411,91	-41,68	424,1
Carregamento Móvel no Bordo	-	-	367,47
Carregamento Móvel no Centro	268,23	64,75	-

Source: Gordilho Neto (2012)

With these values cited by Gordilho Neto (2012), we can calculate the reinforcement using the TQS slab calculator (2023), as shown in figures 20, 21 and 22. Applying $f_{ck}=35\text{MPa}$, $b_w=100\text{cm}$ and $d = 70 - 4 = 66\text{cm}$, we have, for the lower reinforcements:

The value of M_x adopted will be the maximum between the grid analysis method and the Rusch tables.

$$\text{For } M_{x_{\text{grid}}} = 445.23 + 268.28 \text{ (highest value)} = 713.51 \text{ kN.m}$$

$$\text{For } M_{x_{\text{rusch}}} = 411.91 + 268.23 = 680.14 \text{ kN.m}$$

$$\text{For } M_{x_{\text{grate}}} = 463.27 + 367.57 = 830.84 \text{ kN.m}$$

$$\text{For } M_{x_{\text{rusch}}} = 424.10 + 367.47 = 791.57 \text{ kN.m}$$

Therefore, $M_x = 830.84 \text{ kN.m} = 84.72 \text{ tf.m}$ is adopted

$$\text{For } M_{y_{\text{grid}}} = -31.58 - 35.49 = -67.07 \text{ kN.m}$$

$$\text{For } M_{y_{\text{rusch}}} = -41.68 + 64.75 = 23.07 \text{ kN.m}$$

Therefore, $M_{y \text{ sup}} = -67.07 \text{ kN.m} = 6.84 \text{ tf.m}$ and $M_{y \text{ inf}} = 23.07 \text{ kN.m} = 2.35 \text{ tf.m}$

For the Y direction, the calculated reinforcement is lower than the minimum, therefore, it is necessary to adopt the minimum for the design.

For the calculation of negative reinforcement, the maximum negative moment = $-67.07 \text{ kN.m} = 6.84 \text{ tf.m}$ is applied in both directions.

In the same way as the upper reinforcement in the Y direction, the calculated negative reinforcement is lower than the minimum, so it is necessary to adopt the minimum for the design.

Figure 20 - Design of the lower reinforcement in the X direction (parallel to the axis).

Norma: ABNT NBR 6118:2014

Materiais
 f_{ck} : 35 MPa

Geometria / Seção

 b_w : 100 cm
 d : 66 cm

Esforço solicitante (tfm)
 $M_{S_d} = M_{S_k} \times \gamma_f$
 118.61 = 84.72 x 1.4

Flexão simples

Resultados
 $A_s = 44.39 \text{ cm}^2$
 $A_s' = 0.00 \text{ cm}^2$
 $x = 11.4 \text{ cm}$
 $\beta_x = x/d = 0.17$

Armaduras
 44.39 cm²
 A_s : 2 \varnothing 6.3 mm
 \varnothing 6.3 mm c/ 0 cm
 A_s' : 0.00 cm²

$M_{S_d} \rightarrow A_s$
 $M_{R_d} \leftarrow A_s$

Source: Author's own (2023)

Figure 21 - Design of the lower reinforcement in the Y direction (perpendicular to the axis).

Flexão simples

Resultados

$A_s = 1.15 \text{ cm}^2$
 $A_s' = 0.00 \text{ cm}^2$
 Armadura calculada = $1.15 \text{ cm}^2 < \text{Armadura mínima} = 10.28 \text{ cm}^2$
 $x = 0.3 \text{ cm}$
 $\beta_x = x/d = 0.00$

Source: Author's own (2023)

Figure 22 - Design of the upper reinforcement in both directions.

Flexão simples

Resultados

$A_s = 3.35 \text{ cm}^2$
 $A_s' = 0.00 \text{ cm}^2$
 Armadura calculada = $3.35 \text{ cm}^2 < \text{Armadura mínima} = 10.28 \text{ cm}^2$
 $x = 0.9 \text{ cm}$
 $\beta_x = x/d = 0.01$

Source: Author's own (2023)

Using the tables of Pinheiro (2004), it is possible to find the gauge and spacing for each direction, as shown in figure 23.

Figure 23 - Area of the bar section per meter of width (cm²/m).

ÁREA DA SEÇÃO DE BARRAS POR METRO DE LARGURA as (cm ² /m)							
s (cm)	DIÂMETRO NOMINAL (mm)						s (cm)
	6,3	8,0	10,0	12,5	16,0	20,0	
5,0	6,24	10,06	15,70	24,54	40,22	62,84	5,0
5,5	5,67	9,15	14,27	22,31	36,56	57,13	5,5
6,0	5,20	8,38	13,08	20,45	33,52	52,37	6,0
6,5	4,80	7,74	12,08	18,88	30,94	48,34	6,5
7,0	4,46	7,19	11,21	17,53	28,73	44,89	7,0
7,5	4,16	6,71	10,47	16,36	26,81	41,89	7,5
8,0	3,90	6,29	9,81	15,34	25,14	39,28	8,0
8,5	3,67	5,92	9,24	14,44	23,66	36,96	8,5
9,0	3,47	5,59	8,72	13,63	22,34	34,91	9,0
9,5	3,28	5,29	8,26	12,92	21,17	33,07	9,5
10,0	3,12	5,03	7,85	12,27	20,11	31,42	10,0
11,0	2,84	4,57	7,14	11,15	18,28	28,56	11,0
12,0	2,60	4,19	6,54	10,23	16,76	26,18	12,0

Source: Adapted from Pinheiro (2004).

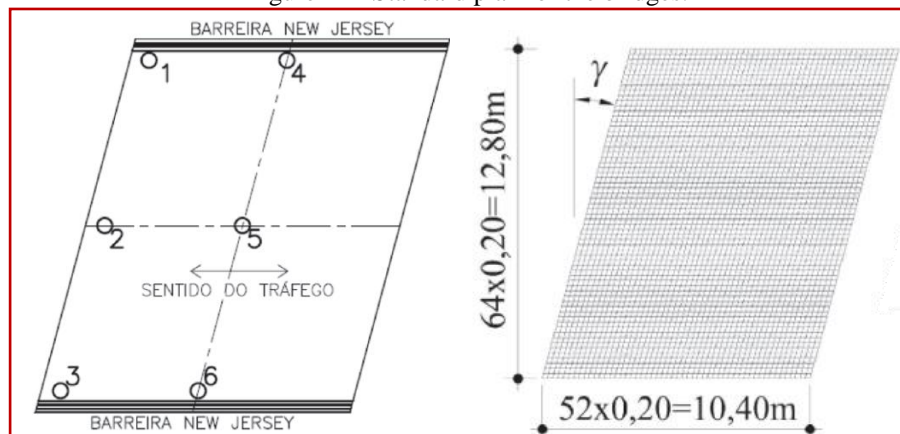
Therefore, we have:

- Parallel to the axis of the bridge: $A_s = 44.39 \text{ cm}^2/\text{m} - \phi 20 \text{ c} / 7 - A_s = 44.89 \text{ cm}^2/\text{m}$.
- Perpendicular to the axis of the bridge: $A_s = 10.28 \text{ cm}^2/\text{m} - \phi 12.5 \text{ c} / 10 - A_s = 12.27 \text{ cm}^2/\text{m}$.
- Both ways, arm. negative: $A_s = 10.28 \text{ cm}^2/\text{m} - \phi 12.5 \text{ c} / 10 - A_s = 12.27 \text{ cm}^2/\text{m}$.

6.1.5 Rocha and Schulz Bridges (2017)

Rocha and Schulz (2017) present a series of concealed slab bridges with a span of 10.40m, a thickness of 0.60m (fixed dimensions) and angles ranging from 0°, 15°, 30° and 45°, forming a total of four bridges analyzed. According to Brasil (2016), since these are isostatic bridges, an adequate pre-dimensioning for the thickness would be $10.40/15 = 0.68\text{m}$, regardless of the angulation, showing that the value adopted by the authors is within the order of magnitude. Rocha and Schulz (2017) adopted six points on the bridge slabs, as shown in figure 24, for the design of the reinforcement through the cracked plate model.

Figure 24 - Standard plan for the bridges.



Source: Rocha and Schulz (2017)

Performing the calculations, Rocha and Schulz (2017) arrived at the values for the reinforcements as shown in the

Table 5. Being The α angle is always zero, since the axis of the slab is always defined in the direction of traffic, and the β angle is defined by $\beta=90^\circ-\gamma$, where γ is the angle of slab sag. The steel areas are presented in a ratio of maximum upper and lower reinforcement, for the direction parallel to the axis (angle α) and to the direction against the axis (angle β)

Table 5 - Steel areas on the slabs.

Ponto	As(α ,sup,máx)/As(α ,inf,máx) - (cm ² /m) - direção paralela ao eixo				As(β ,sup,máx)/As(β ,inf,máx) - (cm ² /m) - direção contrária ao eixo			
	$\gamma = 0^\circ$	$\gamma = 15^\circ$	$\gamma = 30^\circ$	$\gamma = 45^\circ$	$\gamma = 0^\circ$	$\gamma = 15^\circ$	$\gamma = 30^\circ$	$\gamma = 45^\circ$
1	0/12,57	4,1/27,27	8,29/40,78	13,5/48,96	3,69/5,62	8,28/17,18	8,44/35,56	2,8/52,98
2	0/8,17	0/9,15	0,67/18,68	4,92/25,88	0,62/3,27	0,94/5,59	5,72/12,97	11,62/23
3	0/12,57	0/7,89	0/4,03	0/2,54	3,69/5,62	0,87/1,85	0,13/1,42	0,12/0,76
4	0/35,86	0/41,56	0/44,77	0/46,8	0/2,29	0/8,05	0,61/13,34	0,98/18,43
5	0/30,24	0/38,33	0/47,41	0/58,47	0/7,79	0/17,05	0/29,63	0/46,2
6	0/35,86	0/41,56	0/44,77	0/46,8	0/2,29	0/8,05	0,61/13,34	0,98/18,43

Source: Adapted from Rocha and Schulz (2017)

Rocha and Schulz (2017), after calculating the reinforcements, present the rates and total weight of steel for the slab bridges, as shown in the Table 6.

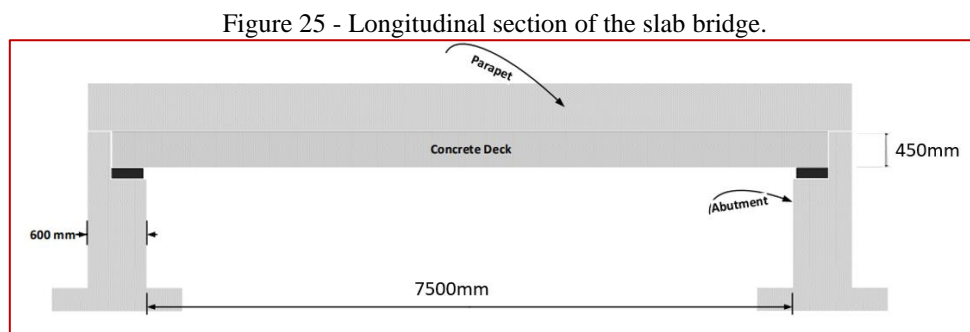
Table 6 - Total weight and steel rates for slab bridges.

γ	Peso total de aço (kg)	Taxas	
		kg/m ²	kg/m ³
0°	7800	59	98
15°	10077	76	126
30°	15153	114	190
45°	23437	176	293

Source: Rocha and Schulz (2017)

6.1.6 Ponte Ajeel (2018)

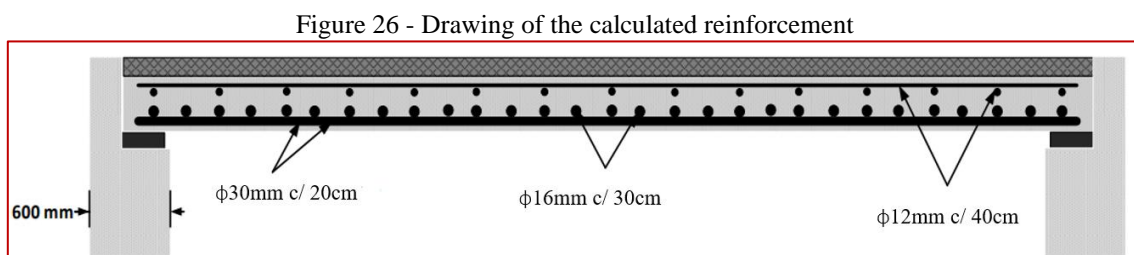
Ajeel (2018) presents a solid slab bridge with a free span of 7.50m, width of 7.30m, supported at the ends by Neoprene devices, forming an isostatic structure. For this free span, Ajeel (2018) adopts a thickness of 0.45m. According to Brasil (2016), for a free span of 7.50m we would have a thickness of $7.50/15 = 0.50\text{m}$, showing that the pre-dimensioning adopted by the author is in the same order of magnitude as recommended. Figure 25 shows the longitudinal section of the bridge.



Fonte: Adapted from Ajeel (2018)

Calculating the reinforcement by dividing the slab into bands, Ajeel (2018) arrived at the following reinforcement values, as shown in figure 23:

- Parallel to traffic (main armature): $\phi 30\text{mm}$ w/ 20cm;
- Perpendicular to traffic (distribution reinforcement): $\phi 16\text{mm}$ w/ 30cm;
- In both directions (negative armor): $\phi 12\text{mm}$ w/ 40cm



Fonte: Adapted from Ajeel (2018)

It should be noted that there are reinforcement diameters slightly different from those of the Brazilian standards because the reference is foreign.

6.1.7 Steel Rates

Using the values of steel area per square centimeter of the bridges analyzed, it is possible to calculate the steel rate used in the slabs (kgf/m³). The methodology used by the author to calculate the steel rate for the Chianca bridge (2016) will be shown.

According to the results of Chianca (2016), we have the reinforcement design mentioned in Table 1. Repeating here:

- Armor in the middle of the plate, X direction: ϕ 25 w/ 15 cm;
- Armor in the middle of the freeboard, X direction: ϕ 25 w/ 12.5 cm;
- Armor in the middle of the plate, Y direction: ϕ 10 w/ 15 cm;

In the case of the Chianca bridge (2016), the X direction is parallel to the axis of the bridge (11.00 m), causing the reinforcement in this direction to be distributed in the perpendicular direction (9.80 m). Similarly, the Y direction is parallel to the width of the bridge (9.80m), causing the reinforcement to be distributed over 11m. With these values, you will find the number of bars for each gauge. The largest reinforcement of the X direction, i.e. 25 c/ 12.5 cm, is adopted here for ϕ the calculation of steel rates.

For the X direction, we have:

$$\frac{980cm}{12,5} = 79 \text{ } \phi \text{ 25 c/12,5cm}$$

For the Y direction, we have:

$$\frac{1100cm}{15} = 74 \text{ } \phi \text{ 10 c/15cm}$$

According to NBR 7480:2007, we have the following nominal steel mass, in kg/m.

Figure 27 – Characteristics of the bars.

Bitola		TIPO	Área de Aço	Peso Linear
mm	pol.	-	cm ²	kg/m
4.2		CA-60	0,14	0,109
5.0	3/16"	CA-60	0,196	0,154
6.3	1/4"	CA-50	0,31	0,245
8.0	5/16"	CA-50	0,5	0,395
10.0	3/8"	CA-50	0,785	0,617
12.5	1/2"	CA-50	1,22	0,963
16.0	5/8"	CA-50	2,01	1,578
20.0	3/4"	CA-50	3,14	2,466
25.0	1"	CA-50	4,91	3,853
32.0	1 1/4"	CA-50	8,04	6,313

Source: ABNT NBR 7480 (2007)



The length of the bars in the Y direction, after subtracting the covering (3.5cm) from both sides and adding a fold of 53cm (slab thickness of 60cm – 2*cob), will be:

$$980cm - (2 * 3,5)cm + (53cm * 2) = 1079cm = 10,79m$$

Similarly, the length of the bars in the X direction will be:

$$1100cm - (2 * 3,5)cm + (53cm * 2) = 1199cm = 11,99m$$

For the X direction, middle of the freeboard, we have:

$$Qtd\ barras * comp * peso\ linear = 79 * 11,99 * 3,853 = 3649,60kgf$$

For the Y, middle direction of the board, we have:

$$Qtd\ barras * comp * peso\ linear = 74 * 10,79 * 0,617 = 492,65kgf$$

Adding the values of the weights, we have a total weight of 4142.25 kgf.

As the dimensions of the slab are 11.00m span, 9.80m wide and 0.60m thick, we have a total concrete volume of:

$$11 * 9,80 * 0,60 = 64,68\ m^3$$

Calculating the steel rate, dividing the weight of the steel, by the volume of concrete, we have:

$$\frac{4142,25kgf}{64,68m^3} = 64,04\ kgf/m^3$$

For the other bridges, the calculations were made in a similar way and are briefly shown in tables 7, 8, 9 and 10. Table 11 provides a summary of the steel weights, volumes, and rates of each bridge. In situations where the length of the bars exceeded the commercial limit of 12m, an amendment was adopted as shown in figure 28, for $f_{ck}=30\text{MPa}$ and CA-50 steel. For the calculation of the Daher bridge (2010), the largest steel area was adopted for the Leonhardt and W&A methods (90°) and non-orthogonal mesh, and the Asy was adopted following the consality of the bridge

Table 7 – Distribution of reinforcement of the Freire bridge (2013)

DADOS	COMP. DISTRIBUIÇÃO (cm)	BARRA	ESP. (cm)	QTD BARRAS	DOBRAS (2 LADOS) (cm)	COMP. BARRA (cm)	PESO LINEAR (kg/m)	PESO (kg)
ARMATURAS DIREÇÃO PARALELA	1270,00	Ø 20 c/ 10 cm	10,00	127,00	56	649	2,466	2032,55
ARMATURAS DIREÇÃO PERPENDICULAR	600,00	Ø 16 c/ 30 cm	15,00	40,00	56	1374 (Com emenda)	1,578	867,27
							TOTAL	2899,82

Source: Author's own (2023)

Table 8 – Distribution of reinforcement of the Daher bridge (2010).

DADOS	ÁREA DE AÇO (cm²)	COMP. DE DISTRIBUIÇÃO (cm)	BARRA	ESP. (cm)	QTD BARRAS	DOBRAS (2 LADOS) (cm)	COMP. BARRA (cm)	PESO LINEAR (kg/m)	PESO (kg)
ARMS. EM X, DISTRIBUÍDAS EM Y	35,90	2300,00	Ø 25 c/ 10 cm	10,00	230,00	96	1054	3,853	9340,44
ARMS. EM Y, DISTRIBUÍDAS EM X	26,94	965,00	Ø 16 c/ 7 cm	7,00	138,00	96	2444 (Com emenda)	1,578	5322,15
ARMS. NEGATIVAS EM X, DISTRIBUÍDAS EM Y	33,34	2300,00	Ø 25 c/ 10 cm	10,00	230,00	96	1054	3,853	9340,44
ARMS. NEGATIVAS EM Y, DISTRIBUÍDAS EM X	10,70	965,00	Ø 10 c/ 7 cm	7,00	138,00	96	2423 (Com Emenda)	0,617	2063,09
								TOTAL	26066,12

Source: Author's own (2023)

Table 9 – Distribution of reinforcement of the Gordilho Neto bridge (2012).

DADOS	COMP. DE DISTRIBUIÇÃO (cm)	BARRA	ESP. (cm)	QTD BARRAS	DOBRA (2 LADOS) (cm)	COMP. BARRA (cm)	PESO LINEAR (kg/m)	PESO TOTAL (kgf)
ARMS. EM X, DISTRIBUÍDAS EM Y	1300,00	Ø 20 c/ 7 cm	7,00	186,00	126	1387 (Com emenda)	2,466	6361,84
ARMS. EM Y, DISTRIBUÍDAS EM X	1200,00	Ø 12,5 c/ 10 cm	10,00	120,00	126	1461 (Com emenda)	0,963	1688,33
ARMS. NEG. EM X, DISTRIBUÍDAS EM Y	1300,00	Ø 12,5 c/ 10 cm	10,00	130,00	126	1361 (Com emenda)	0,963	1703,84
ARMS. NEG. EM Y, DISTRIBUÍDAS EM X	1200,00	Ø 12,5 c/ 10 cm	10,00	120,00	126	1461 (Com emenda)	0,963	1688,33
							TOTAL	11442,34

Source: Author's own (2023)

Table 10 – Distribution of reinforcement of the Ajeel bridge (2018).

DADOS	COMP. DISTRIBUIÇÃO (cm)	BARRA	ESP. (cm)	QTD BARRAS	DOBRA (2 LADOS) (cm)	COMP. BARRA (cm)	PESO LINEAR (kg/m)	PESO (kgf)
ARMS. EM X, DISTRIBUÍDAS EM Y	730,00	Ø 30 c/ 20 cm	20,00	37,00	76	819	5,55	1681,82
ARMS. EM Y, DISTRIBUÍDAS EM X	750,00	Ø 16 c/ 30 cm	30,00	25,00	76	716	1,578	282,46
ARMS. NEGATIVAS EM X, DISTRIBUÍDAS EM Y	730,00	Ø 12 c/ 40 cm	40,00	19,00	76	819	0,89	138,49
ARMS. NEGATIVAS EM Y, DISTRIBUÍDAS EM X	750,00	Ø 12 c/ 40 cm	40,00	19,00	76	799	0,89	135,11
							TOTAL	2237,88

Source: Author's own (2023)

A summary of the steel rates of slab bridges is presented in table 11, separated by orthogonal and hidden bridges. As can be seen, the steel rates of orthogonal bridges are in the order of magnitude of 100 kg/m³, a value cited by Botelho (2004). The hidden bridges, Daher (2010) and Rocha and Schulz (2017) of 30° and 45° of consibility, show that the greater the consibility, in this case, the higher the reinforcement rate.

Table 11 – Summary of the steel rates of the slab bridges studied.

TAXAS DE AÇO			
PONTES ORTOGONAIS	PESO (kg)	VOL (m ³)	TAXA (kg/m ³)
CHIANCA (2016)	4142,25	64,68	64,04
FREIRE (2013)	2899,82	26,67	108,73
GORDILHO NETO (2012)	11442,34	109,2	104,78
(0°) ROCHA E SCHULZ (2017)	7800,00	79,87	97,66
PONTE AJEEL (2018)	2237,88	24,64	90,82
MÉDIA			93,21
PONTES ESCONSAS	PESO (kg)	VOL (m ³)	TAXA (kg/m ³)
DAHER (2010)	26066,12	122,07	213,53
(15°) ROCHA E SCHULZ (2017)	10077,00	79,87	126,17
(30°) ROCHA E SCHULZ (2017)	15135,00	79,87	189,50
(45°) ROCHA E SCHULZ (2017)	23437,00	79,87	293,44
MÉDIA			205,66

Source: Author's own (2023)

Figure 28 – Anchor length (seam) of the reinforcements.

CONCRETO (Fck)	AÇO CA-25	AÇO CA-50	AÇO CA-60
20 MPa	L = 51*Ø	L = 44*Ø	L = 53*Ø
25 MPa	L = 45*Ø	L = 38*Ø	L = 46*Ø
30 MPa	L = 41*Ø	L = 34*Ø	L = 40*Ø

Source: Adapted from Botelho (2004)



7 CONCLUSION

According to the data collection from the works of Chianca (2016), Freire (2013), Daher (2010), Gordilho Neto (2012), Rocha and Schulz (2017) and Ajeel (2018), the recommendations of slab thicknesses of the The 1996 DNIT Special Works Design Manual were in the same order of magnitude.

In addition, the average steel rates of the orthogonal slab bridges studied was 93.21 kgf/m^3 , making this value very close to the 100 kgf/m^3 mentioned by Botelho (2004). The reinforcement of the hidden slabs resulted in higher rates than those of the orthogonal slabs, with an average of 205.66 kgf/m^3 .



REFERENCES

- AJEEL, Awadh E. Design of Slab Bridges. Lecture Notes on Design of Bridges. Faculty of Engineering. Highway & Transportation Eng. Dept – University of Mustansiriyah. Bagdade. Iraque. 2018.
- ANDRADE, Luisa Guida. Avaliação de modelos de carga móvel para projetos de pontes rodoviárias de pequenos vãos. Trabalho de conclusão de curso. Universidade Federal do Rio de Janeiro. Macaé. 2017.
- ASSOCIAÇÃO BRASILEIRA DE NORMAS TÉCNICAS. NBR 7187: Projeto de pontes, viadutos e passarelas de concreto. Rio de Janeiro, 2021.
- ASSOCIAÇÃO BRASILEIRA DE NORMAS TÉCNICAS. NBR 7188: Carga móvel rodoviária e de pedestres em pontes, viadutos, passarelas e outras estruturas. Rio de Janeiro, 2013.
- ASSOCIAÇÃO BRASILEIRA DE NORMAS TÉCNICAS. NBR 7480: Aço destinado a armaduras para estruturas de concreto armado – Especificação. Rio de Janeiro, 2007.
- BRASIL. Departamento Nacional de Estradas de Rodagem. Diretoria de Desenvolvimento Tecnológico. Divisão de Capacitação Tecnológica. Manual de projeto de obras-de-arte especiais - Rio de Janeiro, 1996.
- BOTELHO, M. H. C. Concreto Armado, eu te amo. Vol II. São Paulo. Edgard Blücher, 2004.
- CHIANCA, Lara. Análise e dimensionamento de ponte em laje. Trabalho de conclusão de curso. Universidade Federal da Paraíba. João Pessoa. 2016.
- DAHER, Michel Touma. Ponte em laje esconsa: Análise e dimensionamento à flexão. Trabalho de conclusão de curso. Universidade Federal do Rio de Janeiro. Rio de Janeiro. 2010.
- DEPARTAMENTO AUTÔNOMO DE ESTRADAS DE RODAGEM (DAER). Normas de Projetos Rodoviários. Porto Alegre, 1991.
- EL DEBS, Mounir Khalil; TAKEYA, Toshiaki. Introdução às pontes de concreto. Notas de aula da disciplina SET – 412 (Graduação em Engenharia Civil) – Universidade de São Paulo. São Carlos. 2007.
- FREIRE, Ricardo Gomes Duarte. Análise estrutural de tabuleiros de ponte em laje usando o método de analogia de grelha. Trabalho de conclusão de curso. Universidade Federal de Pernambuco. Recife. 2013.
- GORDILHO NETO, José Carlos. Lajes de pontes – comparações entre Tabelas de Rüsç e Analogia de Grelha de ponte em laje reta. Trabalho de conclusão de curso. Universidade Federal de Pernambuco. Recife. 2013.
- MARCHETTI, Osvaldemar. Pontes de Concreto Armado. São Paulo: Editora Blucher, 2008.



PARSEKIAN, Guilherme Aris. Cálculo e armação de lajes de concreto armado com a consideração do momento volvente. Dissertação de Mestrado em Engenharia de Estruturas. Escola de Engenharia de São Carlos. São Carlos. 1996.

PINHEIRO, Libânio M. Fundamentos do concreto e projeto de edifícios. Escola de Engenharia de São Carlos. Universidade de São Paulo. São Carlos. 2004.

PINHO, Mauro Ottoboni; BELLEI, Ildoni Hélio. Manual de construção em aço – Pontes e Viadutos em Vigas Mistas. Centro de Informação do IBS/CBCA. Rio de Janeiro. 2007.

ROCHA, B. F.; SCHULZ, M. Lajes esconsas em pontes de concreto armado. Revista Ibracon de Estruturas e Materiais. 2017. Vol. 10.

TQS INFORMÁTICA. TQS Estudante. V24. São Paulo, 2023.

VITÓRIO, José Afonso Pereira. Pontes rodoviárias: fundamentos, conservação e gestão. Recife, CREA-PE, 2002.